Engineering Structures 315 (2024) 118448

Contents lists available at ScienceDirect

Engineering Structures

journal homepage: www.elsevier.com/locate/engstruct

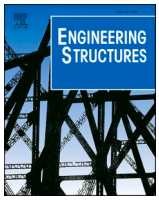

Innovative bridge deck solutions: Examining the impact response and capacity of UHPC with FRP stay-in-place formworks

Emad Pournasiri [a,b], Thong M. Pham [c,*], Hong Hao [a,d,**]

[a] Centre for Infrastructural Monitoring and Protection, School of Civil and Mechanical Engineering, Curtin University, Kent Street, Bentley, WA 6102, Australia
[b] Engineering Department, Parma Composites, 14 Garino Rise, Wangara, WA 6065, Australia
[c] UniSA STEM, University of South Australia, Mawson Lakes, SA 5095, Australia
[d] Guangdong Provincial Key Laboratory of Earthquake Engineering and Applied Technology, Earthquake Engineering Research and Test Centre, Guangzhou University, China

ARTICLE INFO

Keywords:
Stay-in-place formwork
Non-corrosion
Ultra-high performance concrete
Impact loading
Bridge deck
GFRP

ABSTRACT

This study investigates the impact behaviour of bridge decks constructed with ultra-high-performance concrete (UHPC) and fibre-reinforced polymer (FRP) stay-in-place (SIP) formwork. Eight scaled bridge decks were fabricated and tested under pendulum impacts. Two different FRP SIP formwork configurations, i.e., square hollow section (SHS) and Y-shaped stiffened, were considered. Two types of reinforcing bars, i.e., steel and glass FRP (GFRP), were adopted for these samples. The influence of impact velocity on the transient response and progressive damage of the concrete decks under impact loading was investigated. The test results showed that UHPC and Y-shaped stiffeners were effective in decreasing the peak and residual displacements of decks by up to 70 % when compared to decks made with normal strength concrete. UHPC and Y-shaped stiffeners greatly improved the impact and residual impact capacities. The use of GFRP rebars instead of steel reinforcement changed the failure mode and FRP SIP formwork reduced deck damage and mitigated scabbing failure under impact loads. The configuration of FRP SIP formwork had a substantial influence on the impact force and thus the deck's performance. Especially, this study has observed an interesting phenomenon under impact, i.e., reaction force could be greater than impact force, which has not been reported in the literature yet.

1. Introduction

The self-weight of a concrete slab constitutes a substantial proportion of dead load in ordinary reinforced concrete (RC) slab systems. In addition to the heavy load induced on the structure, ordinary RC structures require temporary formwork to retain fresh concrete during construction, which is then removed eventually. A cost analysis for standard concrete structure showed that the cost of a temporary formwork system can exceed half of the construction cost [1], including material and labour costs, which are currently even more expensive due to labour shortages in Australia. To address this issue, the civil construction industry has adopted steel profiled sheets as stay-in-place (SIP) formwork systems for concrete deck slabs, which remain in place structurally integrated with concrete and act as external structural reinforcements throughout the structure's lifecycle (also known as the composite deck). This solution has been adopted widely in the industry and yields great outcomes. However, decks made of steel profiled sheets encountered durability issues such as metal corrosion and structural problems such as crippling and local buckling of the steel parts [2,3].

Advanced composite materials are increasingly being used in civil engineering applications due to their lightweight and non-corrodible property. Among these materials, glass fibre-reinforced polymers (GFRPs) are now being used as SIP formwork for concrete deck slabs. GFRP-concrete composite structures offer the advantages of both materials, making them an excellent choice for modern structures. Bridge decks with GFRP SIP formwork are a new type of composite bridge decks consisting of concrete, GFRP plate, GFRP shear stiffeners and temperature reinforcement [4]. GFRP formworks play a dual role in construction: they act as SIP formwork during the casting of concrete, and they can also function as an alternative to traditional tensile reinforcement,

* Corresponding author.
** Corresponding author at: Guangdong Provincial Key Laboratory of Earthquake Engineering and Applied Technology, Earthquake Engineering Research and Test Centre, Guangzhou University, China.
E-mail addresses: thong.pham@unisa.edu.au (T.M. Pham), hong.hao@curtin.edu.au (H. Hao).

https://doi.org/10.1016/j.engstruct.2024.118448
Received 8 August 2023; Received in revised form 2 May 2024; Accepted 13 June 2024
Available online 28 June 2024

which reduces the deck cross-sectional areas due to the elimination of the bottom concrete cover. Shear stiffeners provide a sufficient shear bond with the concrete so that forming a strong composite action with hardened concrete. Additionally, they can improve the shear capacity of the slab due to their high shear strength [5,6].

In the past decade, several GFRP SIP formwork configurations for decks have been proposed and many efforts have been made to evaluate the performance of this kind of composite deck slabs under quasi-static loads [7–12]. However, during the construction and serviceability phases, bridge decks may suffer from extreme dynamic loading, e.g., impact loading and bouncing of moving vehicles, falling objects, vehicle crash impact, rocks falling, debris flow, shock and impact loads during explosions. It was shown that the dynamic response of a conventional concrete slab is significantly different from that under quasi-static loadings [13]. Therefore, investigating the dynamic responses and failure behaviours of bridge decks with GFRP SIP formwork under impact loading is crucial. Several studies on conventional reinforced concrete slabs under impact loading have revealed that shear failure is the dominant failure mode due to the absence of adequate shear reinforcement within concrete [14–17].

Although investigations on the performance of structures subjected to impact loads are receiving great attention, there are limited studies on such composite deck slabs under impact loading. Emami and Kabir [18] investigated the performance of a series of metal deck composite slabs reinforced by steel temperature bars or reinforced with polymer short fibres under repeated impact loading. The results of the study showed that the slabs exhibited excellent energy absorption capacity and resistance to dynamic loading. More in-depth and quantitative analyses are not yet available. To the authors' best knowledge, there has not been an investigation on the dynamic performance of concrete slabs cast on GFRP SIP formwork under extreme loading yet.

On the other hand, ultra-high performance concrete (UHPC) has been developed using various fibre types, binders, sand types, and chemical additives and has gained significant attention in construction. Through its high compressive, flexural, and tensile strengths, high ductility, toughness and durability, UHPC demonstrates exceptional mechanical properties. The shear weakness in traditional FRP stay-in-place formwork's deck can be overcome by using UHPC to replace normal concrete. Moreover, UHPC is highly durable, use it can reduce maintenance costs during the life of the structure [19–21].

This study considers newly proposed configurations of GFRP SIP formwork featuring a base plate with Y-shape stiffeners or square hollow section GFRP (SHS stiffeners). These configurations were previously introduced and investigated in previous studies [6,22], where it was shown that the use of Y-shape stiffeners in combination with ultra-high performance concrete (UHPC) can significantly enhance the shear resistance and maximum load-carrying capacity of the deck cast into FRP SIP formworks under quasi-static loading.

Considering this research gap and the recent development in the field, this study investigates the structural behaviour of GFRP SIP formwork bridge decks under impact loading. The investigation focuses on two different stiffener configurations and examines the performance of two types of concrete: normal strength concrete and non-metallic UHPC. This prototype will offer a complete-non-metallic SIP formwork bridge deck made of UHPC with great performance and corrosion resistance.

2. Experimental Investigation

2.1. Test specimens and Parameters

The experimental tests involved eight deck specimens, measuring 1405 mm in length and 604 mm in width. These specimens were fabricated at a scale of 1:2.75 from a full-scale concrete bridge deck. Among these specimens, two were designed as control decks and were constructed using conventional reinforced concrete (RC) with a thickness of 75 mm thick as illustrated in Fig. 1. The control decks were reinforced with top and bottom orthogonal layers of steel and GFRP bars, namely DNCS and DNCF, respectively. These decks serve as a benchmark for comparing the performance of other decks. The third deck, named DNSF, with a thickness of 65 mm consisted of GFRP SIP formwork with seven square hollow sections (SHS) stiffeners as shown in Fig. 1. The use of SHS stiffened formwork offers notable environmental and economic advantages, including a 22 % reduction in concrete usage compared to conventional RC decks. This innovative design approach aims to optimize material utilization while maintaining structural integrity.

The fourth deck, illustrated in Fig. 1, resembled Deck DNSF but was stiffened by seven Y-shape stiffeners and was designated as DNYF. The previous study proved that the Y-shape stiffeners could improve the shear resistance of concrete decks with GFRP SIP formwork and provide better mechanical bonding between concrete and SIP formworks [6,22].

The fifth and sixth decks were similar to the first two decks (DNCS and DNCF), except that they used UHPC comprising 2 % synthetic PVA (Polyvinyl alcohol) fibres and were designated as DUCS and DUCF, respectively. Likewise, the design of the seventh and eighth decks was similar to the Decks DNSF and DNYF but employed UHPC as the main material. These two decks were referred to as DUSF and DUYF. For a comprehensive overview of the test matrix, Table 1 provides a summary of the various deck configurations used in the study.

To provide a convenient reference, each specimen was assigned a specific name based on the following convention: the first part, represented by the letter "D", indicates dynamic loading; the second part consists of either letter "N" or "U", that refers to normal strength concrete or UHPC, respectively; the third part is designated by letters "C", "S", or "Y" representing conventional reinforcement, SHS stiffeners, or Y-shape stiffeners, respectively; and the last part consisting of either "S" or "F" indicates the type of top reinforcement as steel reinforcing bars or GFRP reinforcing bars, respectively. The stiffeners spanning the full length of the formworks in one direction, transverse to the direction of traffic, and rebar meshes were provided in the compressive zone for all the decks. The utilised SIP formwork system was not only acting as permanent structural formwork to support construction loads but also completely replacing the bottom layer of rebar reinforcements and eliminated the 10 mm concrete cover at the bottom of the decks. It is worth mentioning that all the decks have the same effective depth as shown in Fig. 1, ensuring consistency in structural dimensions throughout the study.

2.2. Material Properties

2.2.1. Concrete/UHPC

Concrete with a designed 28-day compressive strength of 34 MPa was used. The maximum aggregate size was 10 mm while the slump was maintained at 100 mm. Three standard cylinders (100×200 mm^2) were tested in compression according to ASTM C39 [23] to determine the compressive strength of concrete. To determine the tensile strength of concrete, three standard concrete cylinders (150×300 mm^2) were subjected to a split tensile test according to the ASTM C496 [24]. The conventional concrete had a tensile strength of 3 MPa on the day of testing. In addition, UHPC comprising 2 % synthetic PVA fibres with a compressive strength of 140 MPa and tensile strength of 12 MPa was used in this study. The mix proportion of normal concrete and UHPC are given in Table 2.

2.2.2. GFRP SIP Formwork

The shape, dimensions and other properties of the employed GFRP formworks are given in Fig. 1. SHS GFRP SIP formwork was 600×604 mm^2 with 41.3 mm deep. It consisted of a 3.2 mm thick GFRP plate with seven 38.1 mm pultruded SHS stiffeners spaced at 80 mm and overall cross-section area and moment of inertia of 5060 mm^2 and 1.15×10^6 mm^4, respectively.

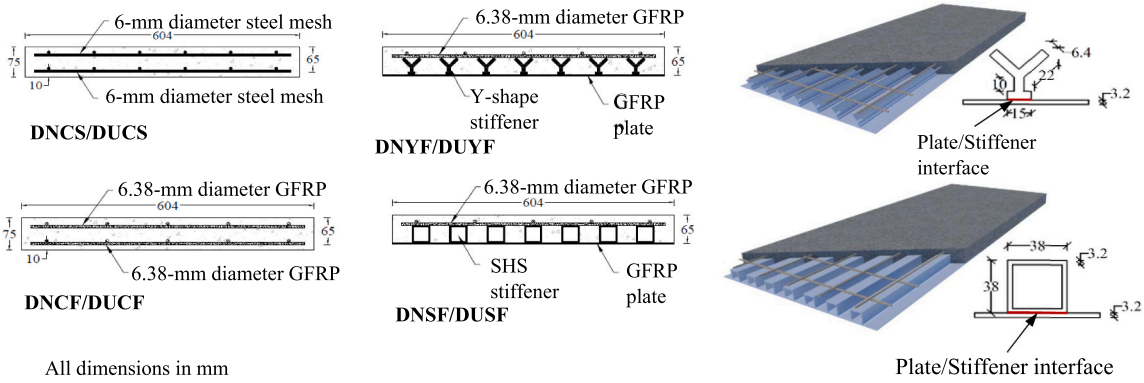

Fig. 1. Stay-in-pace formworks.

Table 1
Summary of the test matrix.

Specimen ID	Overall length (mm)	Clear span (mm)	Width (mm)	Depth (mm)	Reinforcements	
					Bottom	Top
DNCS	1405	665	604	75	Steel mesh	Steel mesh
DNCF	1405	665	604	75	GFRP mesh	GFRP mesh
DNSF	1405	665	604	65	SHS SIP formwork	GFRP mesh
DNYF	1405	665	604	65	Y-shape SIP formwork	GFRP mesh
DUCS	1405	665	604	75	Steel mesh	Steel mesh
DUCF	1405	665	604	75	GFRP mesh	GFRP mesh
DUSF	1405	665	604	65	SHS SIP formwork	GFRP mesh
DUYF	1405	665	604	65	Y-shape SIP formwork	GFRP mesh

Table 2
Mixture proportions of UHPC and normal concrete.

Normal concrete	Weight (kg/m^3)	UHPC constituent	Weight (kg/m^3)
Cement	248.5	Cement	1000
Slag	106.5	Silica fume	250
10 mm aggregate	1015	Silica sand	1100
Sand	809	Water	170
Water	172	Superplasticizer	65
Superplasticizer	1.4	PVA fibre (2 % vol.)	26

Y-shape GFRP SIP formwork was 600 × 604 mm^2 with 40.3 mm deep. It consisted of a 3.2 mm thick GFRP plate with seven 37.1 mm pultruded Y-shape stiffeners spaced at 80 mm and overall cross-section area and moment of inertia of 5075 mm^2 and 0.87 × 10^6 mm^4, respectively. The stiffeners were bonded to the plate using high-strength and low-viscosity epoxy resin after proper surface preparation including sanding and cleaning.

The ultimate tensile strength and modulus of elasticity of FRP stiffeners in the longitudinal direction were 206.8 MPa and 20.7 GPa, respectively. The corresponding properties in the transverse direction were 48.2 MPa and 5.5 GPa, respectively. The ultimate tensile strength and modulus of elasticity of GFRP plates in the longitudinal direction were 165.5 MPa and 13.8 GPa, respectively. In the transverse direction, the corresponding properties were 51.7 MPa and 6.9 GPa, respectively [25].

2.2.3. GFRP rebar

Commercially available size #2 (nominal diameter of 6.4 mm) sand-coated GFRP bars with a nominal cross-sectional area of 32 mm^2 were used as top reinforcement for the decks containing SIP formwork. For the conventional control decks, the same bars were employed as top and bottom reinforcement. According to the manufacturer's specifications based on the nominal cross-sectional area [26], the tensile strength and elastic modulus of the bars were 1100 MPa and 60 GPa, respectively.

2.2.4. Steel rebar

In both the conventional control deck and the deck with UHPC, 6-mm deformed steel bars were utilised as both tensile and compressive reinforcements. To assess the tensile strength of these bars, five coupons were tested in tension according to ASTM A615 [27]. The tensile tests showed a yield strength and modulus of elasticity of 550 MPa and 200 GPa, respectively.

2.3. Fabrication of deck specimens with SIP formwork

The GFRP SIP formwork was placed in the middle of a special wooden formwork as shown in Fig. 2. SHS stiffeners were obstructed by polystyrene foam to avoid penetration of fresh concrete in the hollow sections. The interior of the GFRP SIP formwork was roughened using sandpaper and wiped clean with alcohol. A thin layer of epoxy adhesive was then applied to bond concrete and formwork approximately 20 min before pouring wet concrete on GFRP SIP formwork. Before casting, the top GFRP rebar mesh was placed and secured on the SIP formwork. The decks with UHPC were transferred to the steam curing room after 24 h and conditioned for 3 days at 85 °C.

2.3.1. Epoxy Adhesives

A two-part epoxy was used for bonding GFRP stiffeners to the plate and for bonding fresh concrete to the GFRP SIP formwork. The epoxy had high modulus, high strength, and low viscosity. The physical properties of cured epoxy are summarised in Table 3 [28].

2.4. Test Setup and Instrumentation

The details of the impact experimental program are presented in Table 4. The impact load was applied at the centre of the decks by a pendulum system. Fig. 3 shows the pendulum impact system and all measuring equipment. The system comprised a large steel frame rigidly fixed on a strong solid floor to support the entire testing rig. The pendulum has a long steel arm (75 ×75 ×6 SHS C450) of 2.5 m, and the total weight of the impactor is 593 kg including the arm weight made of solid steel. A 250-kN impact load cell with a striking surface of 50 mm in diameter with a hemispherical nose (diameter of 500 mm) was fixed to the front of the impactor to measure the impact force.

To continue from earlier studies [6,22], a 91 × 91 × 12.7 mm

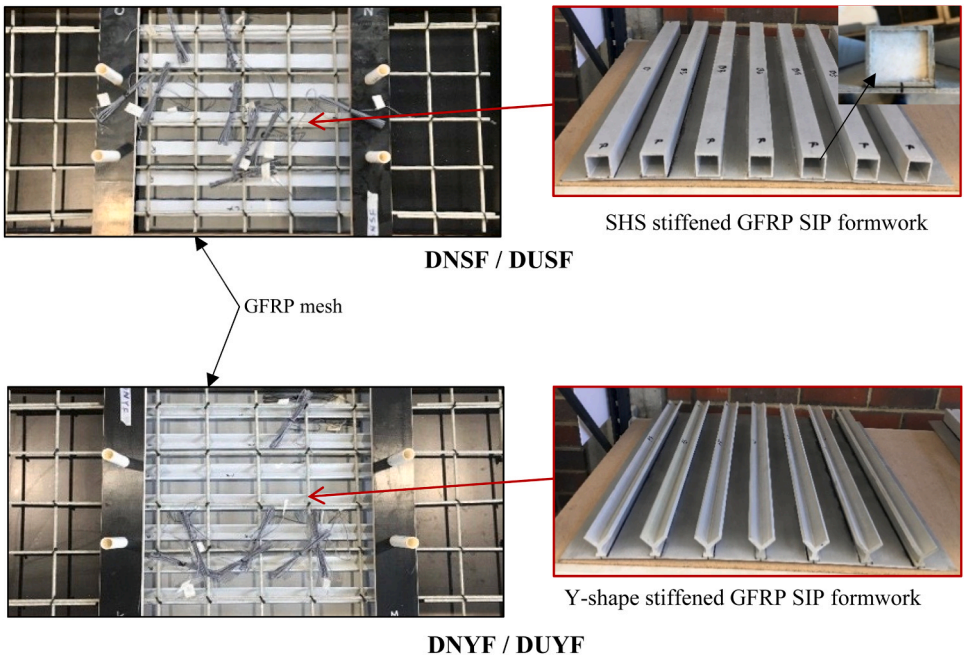

Fig. 2. Top view of the deck specimens with SIP formworks.

Table 3
Physical properties of cured epoxy.

Properties	Value
Compression yield	78.6 MPa
Tensile strength	54.5 MPa
Tensile elongation	3.4 %
Tensile modulus	2.8 GPa
Flexural strength	97.2 MPa
Flexural modulus	3.1 GPa
Bond Strength	50.5 MPa

Table 4
Pendulum impact loading protocol.

Impact	Angle (degree)	Mass (kg)	Velocity (m/s)	Kinetic energy (kJ)	Impact momentum (kg. m/s)
1	10	593	0.9	0.22	516
2	20	593	1.7	0.88	1026
3	30	593	2.6	1.96	1524
4	35	593	3	2.65	1773
5	40	593	3.4	3.43	2016

neoprene rubber pad was placed between the impactor and the concrete surface. This replicated the precise testing conditions from the previous studies, creating a soft-impact loading scenario akin to rubber tires on a road surface. According to the manufacturer, these rubber pads had the ultimate tensile strength of 17 MPa, elastic modulus of 3.8 MPa, and shear modulus of 0.9 MPa [29]. Similar to the previous studies [6,22], to prevent rebounding upon impact and ensure a solid connection between the deck and girders, two reinforced steel beams, 454 mm deep and 190 mm wide, were anchored to the ground using 20 mm diameter high-strength threaded rods. These beams, with 12 mm thick web and flanges, were reinforced with three 12 mm plates on each side and 16 mm steel plates on the top flange to achieve a 540 mm clear span (see Fig. 4).

Finally, steel square hollow sections clamped the deck with eight 20-mm threaded rods. Four 200 kN barrel load cells under each support recorded both positive and negative reaction forces. It is worth noting that positive reaction opposes impact force, negative aligns with it. A 5 kN preload was applied on each bolt to make sure that the barrel load cells were always in compression to be able to monitor both positive and negative reaction forces [30].

The pendulum was raised by a 1.5-Ton winch to reach a designed height, corresponding to a desired angle as described in Table 4. The desired angle was measured by using a protractor which was located on the impactor. Then, the impactor was released to hit the deck at the mid-span. Once the impactor hit the deck and rebounded, it was pulled back manually by holding a rope connected to the impactor to avoid a second impact.

The decks were tested under sequential impacts with increasing impact velocities while maintaining a constant mass. The impact velocity was gradually increased by increasing the lifting angle at 10° intervals till the deck failed. Laser triangulation sensors were placed at mid-span to monitor the displacements. Load cells, SGs and laser triangulation sensors were connected to a data acquisition system at a sampling rate of 19.2 kHz. A high-speed camera was set up to monitor the failure progress of the deck. Displacement traced by using digital image correlation software (DIC) was used to confirm the displacement recorded by laser triangulation. The camera was set to capture 20,000 fps (frame per second).

Table 4 summarizes the release angle (θ) of the impactor and impact velocity for each impact. The design velocity of the pendulum hammer can be calculated by using Eq. (1):

$$v = \sqrt{2g \times L \times (1 - Cos(\theta))} \quad (1)$$

where g is the acceleration of gravity and its value is 9.81 m/s^2, L is the length of the pendulum arm, and θ is the release angle from the vertical axis.

3. Experimental results and discussion

3.1. Crack patterns and failure

3.1.1. Normal concrete decks reinforced with conventional steel/GFRP bars

Damage of the decks after each impact test is shown in Fig. 5. Decks DNCF and DNCS exhibited global flexural response under the first two impacts. However, their response to the last impact (2.6 m/s) differed

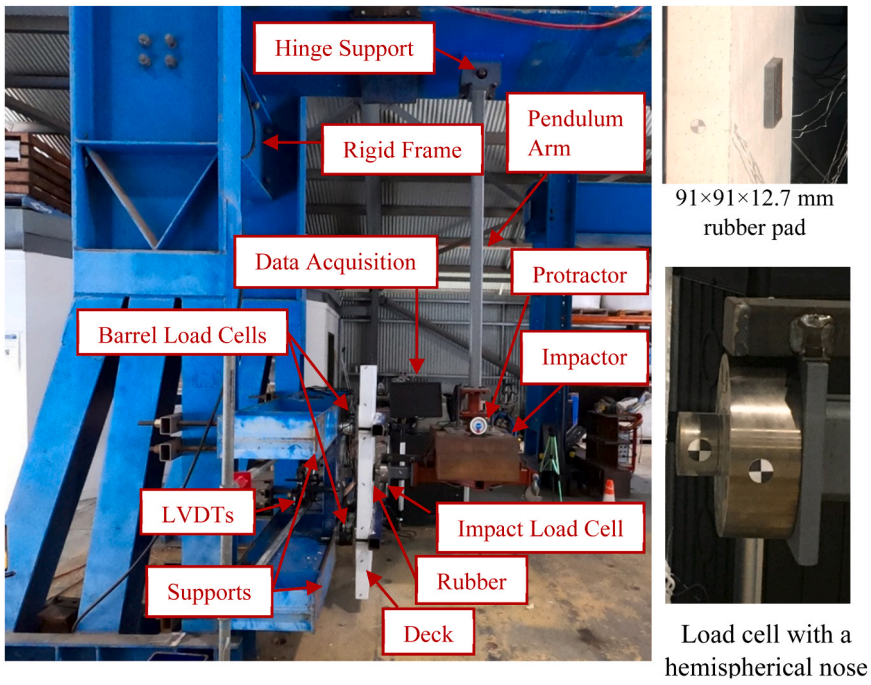

Fig. 3. Test setup for pendulum impact tests.

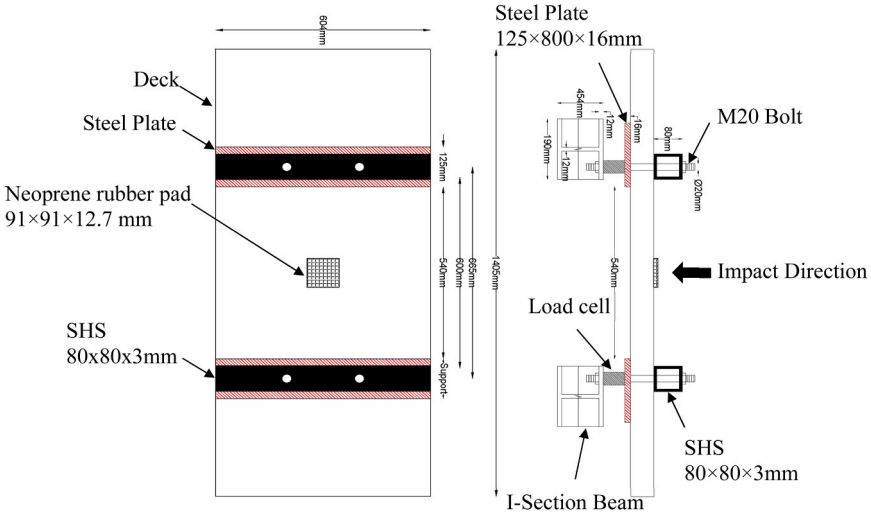

Fig. 4. Schematic diagram of the test decks.

significantly. After the initial impact test with a velocity of 0.9 m/s, a minor flexural crack was observed at the soffit of Deck DNCF. Under the second impact test with a velocity of 1.7 m/s, global cracks were radiated from the impact point at the tension face of the deck. Notably, as these cracks propagated through the deck thickness, there was no evidence of concrete scabbing or impactor penetration. However, the subsequent impact at a velocity of 2.6 m/s led to pronounced punching and impactor penetration. Localized punching failures were coupled with concrete scabbing and concrete spalling at the bottom and top surfaces of the deck, respectively.

During the initial impact, Deck DNCS showed no crack during the first impact. However, after the second impact (1.7 m/s), cracks originated underneath the loading point at the tension face of Deck DNCS. The cracks propagated transversely along the width of the deck towards the free edges of the deck. The subsequent impact at a velocity of 2.6 m/s led to both concrete scabbing and flexural damage, which developed outside of the impact region and stemmed from cracks developed under prior impacts. The flexural failure of the deck was coupled with impactor penetration and concrete scabbing.

The overall crack patterns at the tension face of Decks DNCF and DNCS were similar. Fewer but wider cracks were observed in the deck reinforced with steel before failure, compared to the deck reinforced with GFRP bars, where smaller cracks were observed. This indicates the difference in bond characteristics between steel and GFRP sand-coated bars. The sand-coated surface of GFRP bars with additional adhesive bonds resulted in more uniform distribution of stress and thus finer cracks distributed along the bar length. On the other hand, steel bars with a deformed ribbed surface resulted in wider cracks.

From a comparison of the severity of damage at the bottom surface of Decks DNCS and DNCF, it can be concluded that the deck with steel reinforcement experienced both scabbing and penetration, while using GFRP reinforcement increased concrete scabbing and changed the failure mode from mainly flexural failure to punching failure. Similar behaviour was also reported for the same decks under static loads except

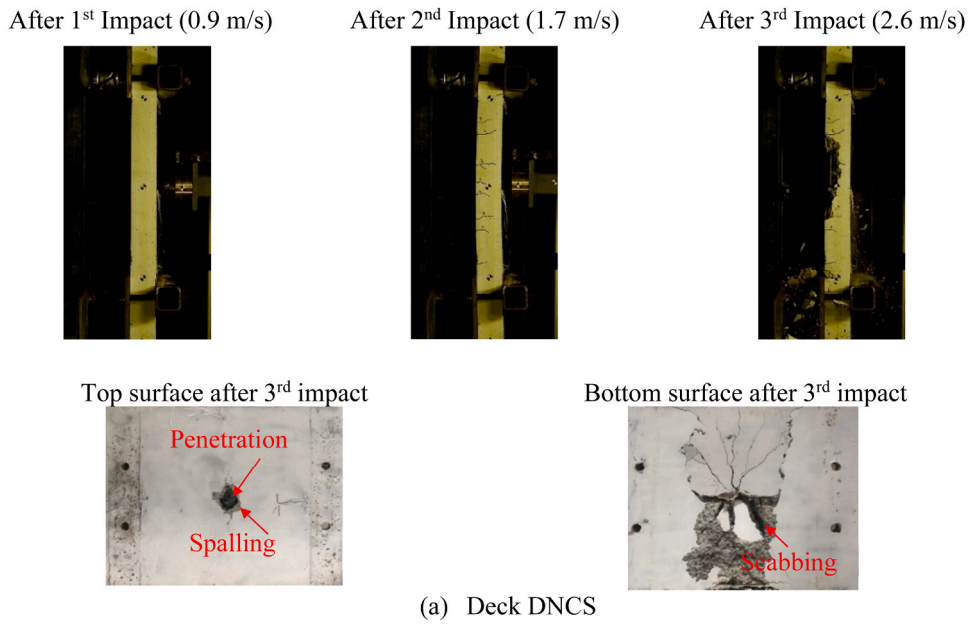

Fig. 5. Crack pattern of the normal concrete decks with conventional steel/GFRP meshes.

scabbing [22].

The ultimate behaviour of the deck reinforced with steel bars was primarily governed by its flexural strength. However, the failure mode changed from flexural failure to punching shear failure by replacing steel bars with GFRP bars. This phenomenon is due to the higher tensile strength and lower dowel action of the GFRP bars as compared to the steel bars. The higher tensile strength increased the flexural strength while the low dowel action of GFRP bars reduced the shear strength of Deck DNCF as compared to the deck reinforced with steel bars. It is worth mentioning that a weaker bond between the GFRP bars and the surrounding concrete than the bond between steel bars and concrete also led to severe damage at the bottom surface of Deck DNCF. Observations of decks showed that normal concrete decks failed by flexural failure. The use of FRP reinforcement led to the change of failure mode from flexural to punching shear.

3.1.2. Normal concrete decks reinforced with FRP SIP formwork

The decks with FRP SIP formworks, Decks DNSF and DNYF, did not show any crack or deformation at the initial impact load at 0.9 m/s. When the impact velocity increased, only a few minor flexural cracks were noticed at the tension face of the decks. However, as the impact tests were continued, significant perforated damage became apparent, including slight debonding between the concrete and GFRP plates, see Fig. 6. A comparison with static loading tests indicated similar behaviour and both the decks failed in punching shear [22]. Compared to the reference decks, these decks with SIP formwork suffered significantly less damage associated with only a minor flexural crack while no scabbing was observed, proving the advantage of using SIP formwork in mitigating scabbing failure under impact loads.

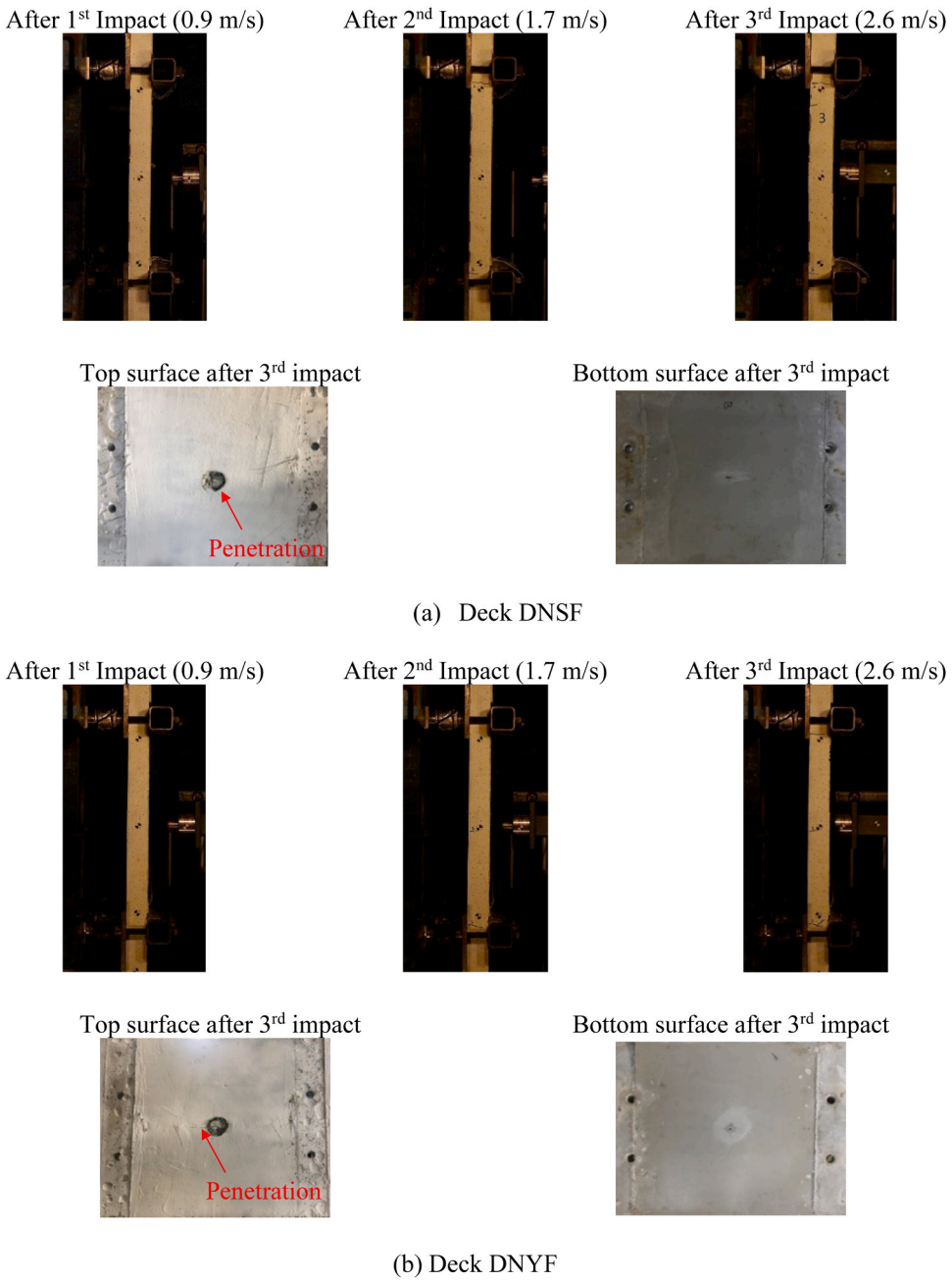

Fig. 6. Crack pattern of the decks with SIP and normal concrete.

3.1.3. UHPC decks reinforced with conventional steel/GFRP bars

A similar pattern emerged for Decks DUCS and DUCF, in which the normal concrete was replaced by UHPC. Wider and fewer cracks were observed in the deck reinforced with steel bars (DUCS) while the number of cracks on the deck reinforced with GFRP bars (DUCF) was higher and more uniform. Both the decks experienced minor crushing of the concrete cover on the top surface at the impact point before failure, as shown in Fig. 7.

During impact, flexural cracks were predominantly observed in Deck DUCS, propagating from the tensile region throughout the height of the deck. These cracks were primarily concentrated near the impact zone. However, for Deck DUCF, more flexure-shear cracks were observed closer to the supports. When the beam was subjected to the 5th impact with a velocity of 3.4 m/s, localized concrete scabbing was observed for Deck DUCF while a global flexural failure was observed for Deck DUCS.

Negative moment cracks were also observed on the top face of both decks. As reported by Pham, et al. [31] the formation of plastic hinges and large inertial force can be the reason for these negative moment cracks. The crushing of the concrete cover was symmetric under the impact area, with the localized punching of the concrete cover to one side of the impact point.

In the previous study [6], it was reported that the ultimate behaviour of the UHPC deck reinforced with steel bars was primarily governed by its flexural strength under static loading. Shallow cracks were observed for the UHPC decks as compared to the normal concrete decks. Unlike Deck DUCS, the failure of the UHPC deck reinforced with GFRP bars under static loading was governed by a critical diagonal crack farthest from the midspan led to a sudden shear failure of the deck.

The failure behaviours of these two decks under impact loading resembled that under static loads. The use of UHPC significantly reduced cracking and scabbing failure, e.g., no scabbing for Deck DUCS while scabbing of Deck DUCF only happened at a lot higher impact velocity as

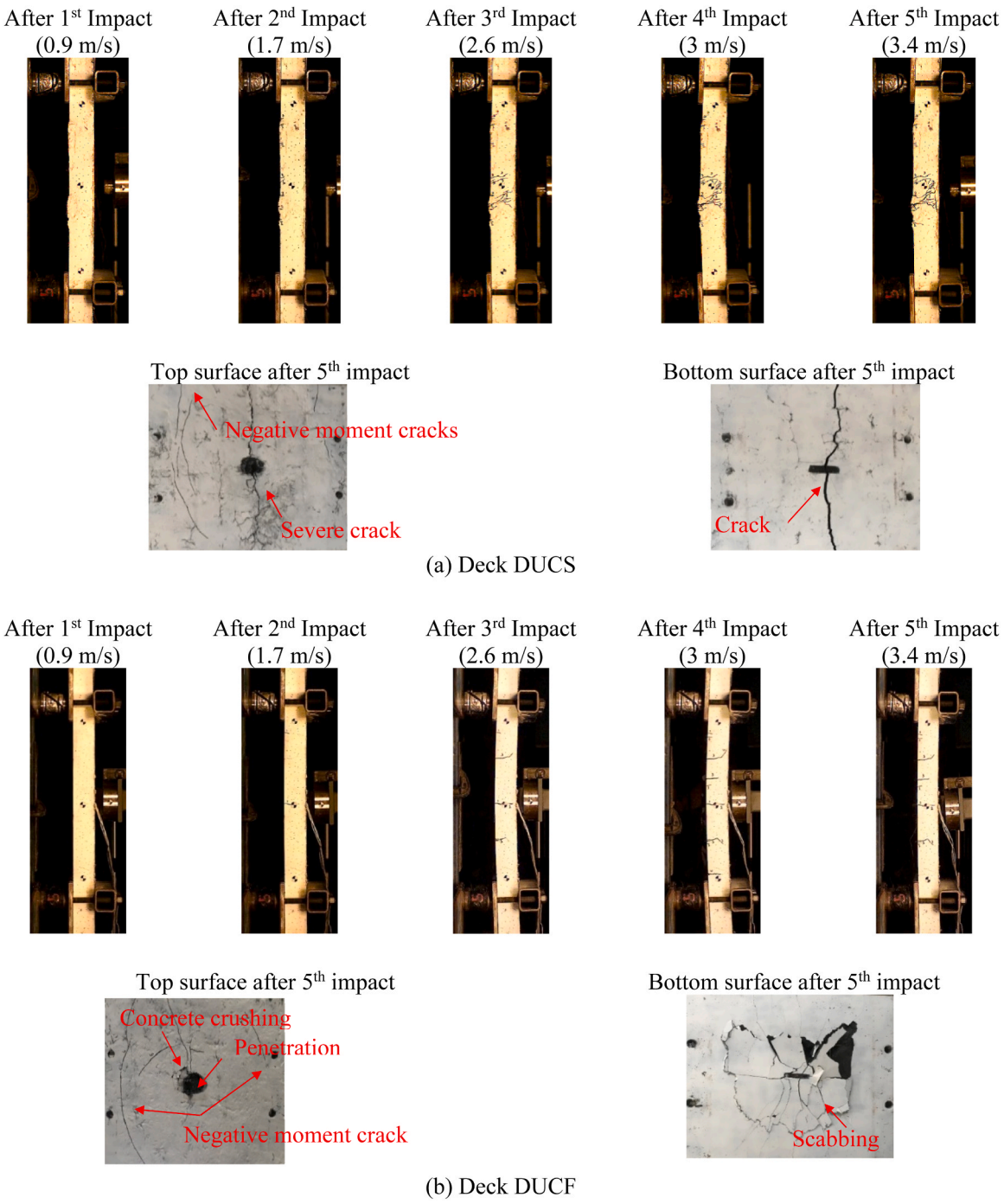

Fig. 7. Crack pattern of the UHPC decks with conventional steel/GFRP meshes.

compared to that of Deck DNCF.

3.1.4. UHPC decks reinforced with FRP SIP formwork

Similar to Decks DNSF and DNYF, no crack was observed on the UHPC decks with FRP SIP formworks after the 1st impact at a velocity of 0.9 m/s. The first crack appeared in the middle of Deck DUSF at the 2nd impact test (see Fig. 8). Subsequently, localized perforated damage was observed at the 3rd impact with a velocity of 2.6 m/s. As expected, Deck DUYF showed better performance under impact tests and the first crack appeared at the 3rd impact and the deck failed with the impactor penetrating into the deck at the 4th impact (3 m/s). More flexural-shear cracks appeared closer to the support regions followed by localized concrete punching at subsequent impact.

3.2. Impact force time history

The time histories of the impact and total reaction forces of all the decks are shown in Fig. 9. It is obvious that the peak impact force increased with the impact velocity before major damage. Upon impact, the impact force experienced a sharp increase, followed by a significant drop. This behaviour could be attributed to the occurrence of flexural cracks, which led to a reduction in stiffness and deck acceleration. Fig. 10 shows the start point of the midspan displacement coincided with the peak impact force. Initially, there was no displacement, and only the impact force gradually increased from zero to its peak value. During the impact, the deck encountered an impulsive force, and its response was influenced by its inertia, which refers to its resistance to transitioning

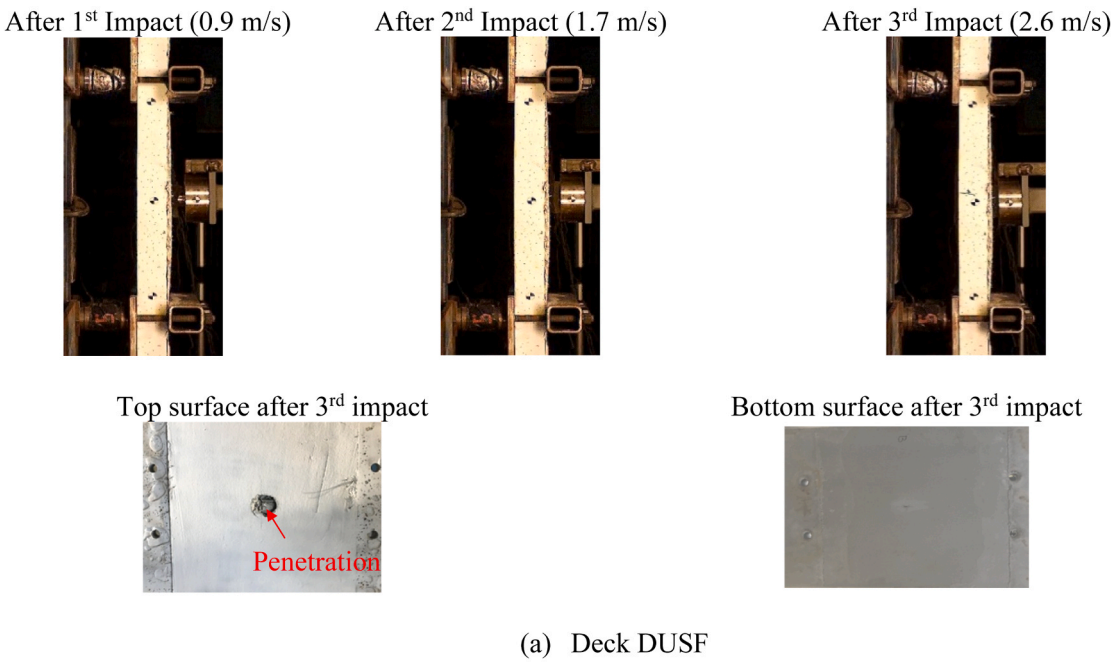

Fig. 8. Crack pattern of the UHPC decks with SIP formworks.

from rest to motion.

The impact force experienced by concrete structures under impact loading has been extensively studied [31–34]. It has been established that the local stiffness, comprising the contact stiffness and local shear stiffness, plays a significant role in governing this force, particularly concerning punching failure[32,35]. The contact stiffness is dependent on both the contact area and the elastic modulus of the impacted structures. The contact area between the impactor and the decks remained constant in this study, therefore, the contact stiffness is affected by the elastic modulus of concrete and the interlayer. In addition, the local shear stiffness and shear resistance were governed by the properties of concrete and reinforcement. Accordingly, the impact force profile of these decks can be explained based on these mechanisms.

3.2.1. *Influence of conventional reinforcement*

Impact test results showed that GFRP reinforcing bars generally reduced the peak impact force due to lower shear resistance of FRP as compared to steel bars. For example, under the impact velocity of 1.7 and 2.6 m/s, Deck DUCS exhibited a peak impact force of 94.8 and 142 kN, respectively, while the peak impact forces of Deck DUCF experienced are 9 % and 27 % lower at the same impact velocities, i.e., 86.7 kN and 104 kN, respectively. These findings indicate that the use of FRP reinforcement resulted in slightly lower impact resistance than steel reinforcement mesh for the decks subjected to impact loads.

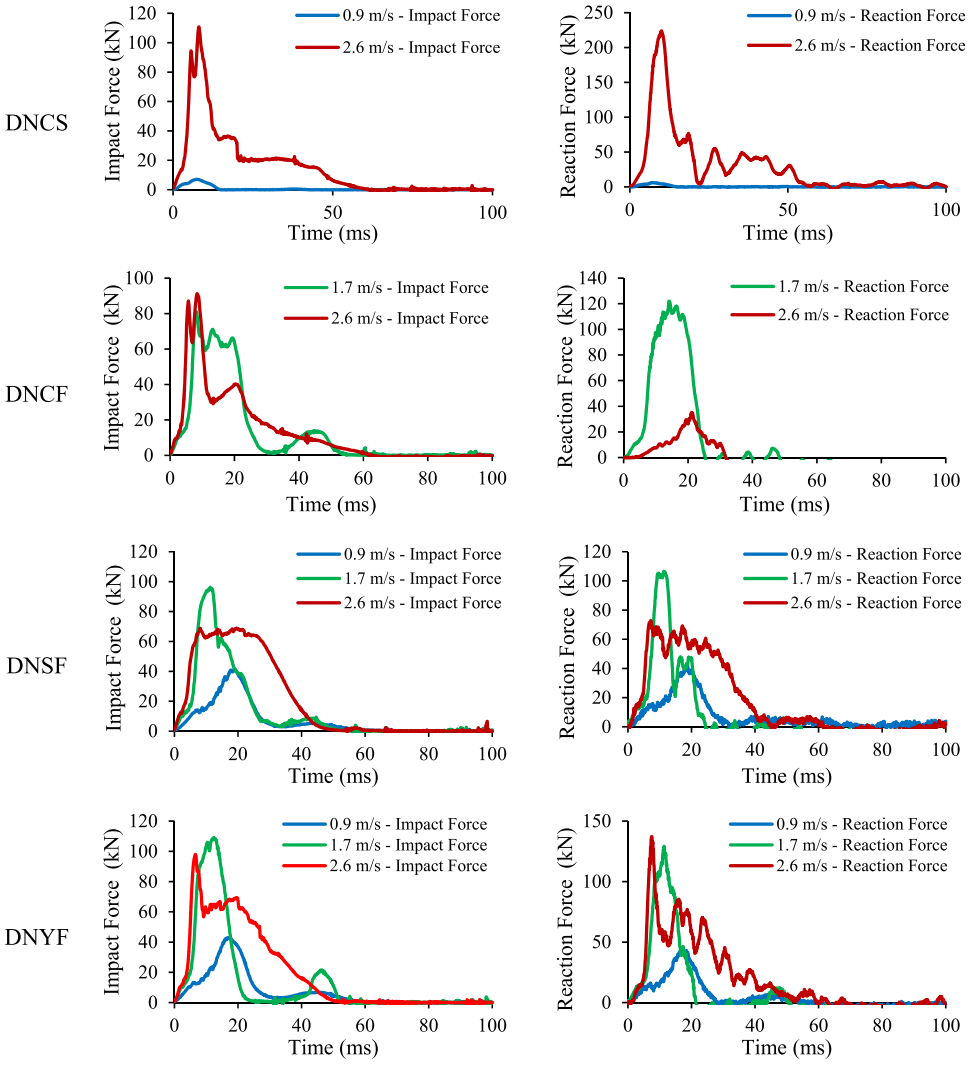

Fig. 9. Impact and reaction forces–time histories of the tested decks.

3.2.2. *Influence of UHPC*

UHPC has significantly higher modulus as compared to normal concrete. Consequently, the decks with UHPC are expected to have higher contact stiffness than those made of conventional concrete. Furthermore, concrete structures subjected to impact loads are susceptible to punching shear failure at a specific impact velocity [30,36]. The use of UHPC and SIP formwork is expected to greatly improve the shear strength and shear stiffness of the decks. These improvements can be attributed to the properties of UHPC and the performance of the SIP formwork system. These observations from the previous studies are helpful to explain the observed behaviours in this study.

As expected, the impact force of the decks made of UHPC was generally higher than those made of normal-strength concrete. Decks DUCS and DUCF made with UHPC exhibited 28 % and 14 % higher peak impact force than Decks DNCS and DNCF made with normal strength concrete at the impact velocity of 2.6 m/s, respectively. This phenomenon is mainly due to the higher contact stiffness and shear stiffness of UHPC which led to better performance under impact loads.

3.2.3. *Influence of FRP SIP formwork and Stiffener's geometry*

A similar trend was also observed for the decks with FRP SIP formworks. The results showed that the peak impact force of Decks DNSF and DNYF was 19 % and 35 % higher than Deck DNCF at the impact velocity of 1.7 m/s. Likewise, 14 % and 74 % increments were observed in Decks DUSF and DUYF as compared to Deck DUCF at the impact velocity of 2.6 m/s. These findings emphasis the significant benefits of using FRP SIP formworks in improving the impact resistance of concrete decks.

In addition, the impact force-time histories of the decks with FRP SIP formwork revealed the significant influence of Y-shaped ribs on the impact resistance. For example, when the impact velocity was 2.6 m/s, Decks DNYF and DUYF exhibited 42 % and 53 % higher impact force as compared to the corresponding Decks DNSF and DUSF, respectively. This indicated that the shear stiffness of the decks with Y-shape FRP SIP formwork is significantly higher than those with SHS stiffeners. These findings align with previous studies, which emphasized the superior shear resistance provided by Y-shaped stiffeners [6,22]. The presence of Y-shaped ribs in the SIP formwork contributes to the improved shear stiffness observed in this study. Consequently, the decks incorporating FRP SIP formwork demonstrated enhanced impact resistance, as evidenced by the higher impact forces.

Comparison of FRP SIP formwork and UHPC showed that the peak impact force of Decks DUSF and DUYF was 72 % and 85 % higher than Decks DNSF and DNYF at the impact velocity of 2.6 m/s even though the cross-sectional area of these two stiffeners was relatively similar. However, this corresponding increment was reduced to 7 % and 10 % at the impact velocity of 1.7 m/s. These findings highlight the advantages of

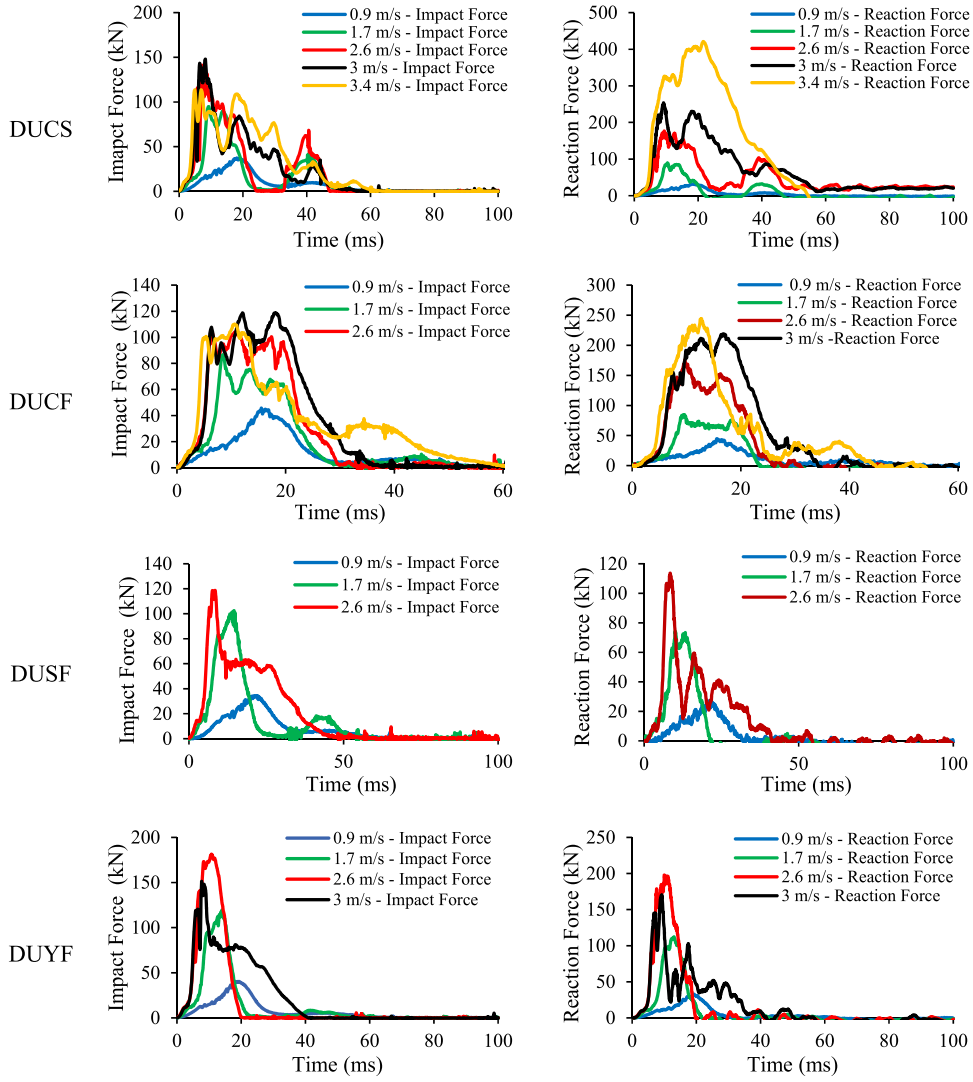

Fig. 9. (*continued*).

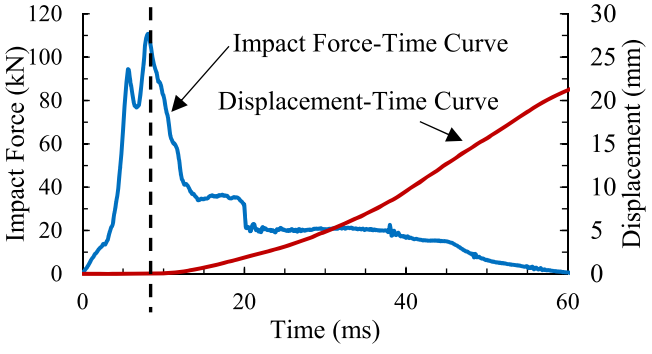

Fig. 10. Typical impact force-time and displacement-time histories of the decks.

utilizing UHPC and FRP SIP formworks in enhancing the impact resistance of concrete decks.

3.3. Reaction force time history

The time histories of the reaction forces of all the decks are shown in Fig. 9, where the reaction force is the sum of all eight barrel load cells at the two supports. Similar to the impact force, the peak reaction force also increased with the impact velocity until reaching its capacity. The short time lag between the impact force and the reaction force can be attributed to two factors. Firstly, due to the relatively short span of the decks, the impact load was rapidly transferred from the centre to the supports. Secondly, the decks were designed to be monolithically connected to the girder, facilitating the immediate transmission of applied forces to the supports. Consequently, all test specimens exhibit high-value support reactions with a minimal time lag.

The impact force-time histories of the decks with FRP SIP formwork demonstrated the significant influence of Y-shaped ribs on the reaction force. For example, when the impact velocity was 1.7 m/s, Decks DNYF and DUYF exhibited 16 % and 35 % higher reaction force as compared to Decks DNSF and DUSF, respectively, indicating the higher impact resistance of the decks with Y-shape stiffeners.

Interestingly, this study observed that the reaction force of decks could be higher than their impact force when subjected to high impact velocities. A thorough and careful check against the test setup, equipment and data acquisition system was carried out to ensure the recorded signals were reliable. This phenomenon has not been reported in the literature yet.

It is understood that when a structure is struck by an object and induces an impact force, the impacted structure resists this impact force through its loading resistance and its inertia resistance [34,37,38]. The

impact force is equal to the sum of the reaction force and the inertia resistance although their values change over time. Accordingly, the reaction force should be smaller than the impact force. The experimental results from this study consistently showed that the reaction force of these decks was higher than the corresponding impact force under high impact velocities. All structures must always satisfy the equilibrium condition, from the relationship above, the inertia force in these decks might act in the same direction as the impact force. As a result, the reaction force is equal to the sum of the impact force and inertia force.

This phenomenon suggests that considering the same mass and stiffness for a deck, a high impact velocity associated with high impact energy might have triggered high vibration modes. Consequently, the vibration of the decks fluctuates substantially in both magnitude and direction. As a result, there can be a moment when the impact force and inertia force are in the same direction, which will cause a higher reaction force. This is a very interesting phenomenon. Numerical simulation may help to unveil the mechanism behind this observation, which has been carrying out and will be reported in a future study. More research efforts are highly sought to confirm as well as unveil this phenomenon.

3.4. Displacement

The maximum and residual lateral displacement of all the tested decks are tabulated in Table 5 while their displacement time histories are plotted in Fig. 11.

3.4.1. Influence of conventional reinforcement

The displacement-time histories of the UHPC decks show that using GFRP reinforcing bars generally resulted in larger maximum and residual displacements as compared to using steel reinforcement. When subjected to impact loading, it has been found that FRP-reinforced UHPC decks underperformed as compared to the steel-reinforced counterparts. For example, under the impact velocity of 1.7 m/s, Deck DUCF exhibited a displacement of 3.3 mm, while the displacement of Deck DUCS was lower at 2.3 mm. When the impact velocity increased to 3 m/s, Deck DUCF had a displacement of 9.4 mm, while Deck DUCS had a 20 % lower displacement of 7.7 mm. These findings suggest that the use of FRP-reinforced UHPC decks provided lower impact resistance than steel-reinforced UHPC decks. The maximum difference in the residual displacement was 64 % between Decks DUCS and DUCF, which can be attributed to the lower elastic modulus of FRP as compared to steel.

3.4.2. Influence of concrete

The maximum and residual displacement of the decks made of UHPC were substantially smaller than their counterparts made of normal strength concrete due to high modulus and small crack width of UHPC. For example, Decks DUCS and DUCF made of UHPC exhibited 73 % and 71 % smaller displacement than Decks DNCS and DNCF made of normal strength concrete, respectively. This remarkable reduction in the displacement can be attributed to the beneficial influence of fibres, which proves the good stiffness and resistance of UHPC under impact loads. In addition, the UHPC decks also experienced lower penetration of the impactor, resulting in reduced concrete spalling and scabbing when compared to the decks made with normal-strength concrete.

3.4.3. Influence of FRP SIP formworks

The use of FRP SIP formwork greatly minimized the displacement of the decks as shown in Table 5. Deck DNYF with Y-shape stiffeners had the maximum displacement of 1.8 mm, which was 54 % smaller than that of Deck DNCF at 3.9 mm when the impact velocity was 1.7 m/s and the residual displacement was 65 % smaller, i.e., 0.7 mm vs 2 mm. Similarly, under the impact velocity of 2.6 m/s, Deck DNYF exhibited a lower displacement of 15.5 mm compared to Deck DNCF with a displacement of 22.2 mm. This indicates that the use of Y-shaped FRP SIP formwork in UHPC decks could improve the impact resistance, particularly when compared to FRP-rebar reinforced UHPC decks under high-velocity impact. The difference in the displacement between the two decks was approximately 30 %.

On the other hand, both Decks DNCF and DNSF exhibited a similar displacement under the impact velocity of 1.7 m/s. However, by increasing the impact velocity, the influence of using FRP SIP formwork became obvious. Replacing tensile GFRP bar reinforcement with SHS stiffened SIP formwork of Deck DNSF reduced the maximum

Table 5
Results of impact tests.

Specimen	Impact velocity (m/s)	Peak impact force (kN)	Time at peak impact force (ms)	Peak displacement (mm)	Time at peak displacement (ms)	Residual displacement (mm)	Mid-span strain (μm/m)
DNCS	0.9	7	7.50	0.05	36.35	0	2584
	2.6	110.7	8.10	23.1	58.86	20	-
DNCF	1.7	81.1	8.10	3.9	34.86	2	12319
	2.6	91.2	8.37	22.2	58.11	-	-
DUCS	0.9	37.5	18.06	0.3	50.04	-	668
	1.7	94.8	9.20	2.3	48.99	1.5	-
	2.6	142	7.07	6.3	47.96	4.5	-
	3	148	8.22	7.7	137.62	7.7	-
	3.4	113.6	6.88	17.3	56.25	-	-
DUCF	0.9	45.8	16.54	0.3	49.14	0.1	1429
	1.7	86.7	9.18	3.3	47.33	1.8	-
	2.6	104	10.52	6.4	43.92	1.6	-
	3	118.7	11.60	9.4	44.05	1.6	-
	3.4	110.2	10.83	29.1	58.59	17.2	-
DNSF	0.9	41.4	18.25	0.4	44.76	0.1	1008
	1.7	96.2	11.92	3.2	48.94	2	4330
	2.6	68.9	19.68	16	52.20	10.2	6556
DNYF	0.9	42.9	17.42	0.5	50.33	0.2	1454
	1.7	109.1	11.58	1.8	44.51	0.7	4878
	2.6	98	7.36	15.5	54.39	10	6915
DUSF	0.9	34.4	22.19	0.4	50	0.2	452
	1.7	102.5	14.57	1.1	45.35	0.4	1848
	2.6	118.7	8.46	10.4	51.58	6	3677
DUYF	0.9	40.4	19.31	04	47.96	0.05	361
	1.7	119.5	14	1.1	44.83	0.35	3403
	2.6	181.4	10.73	2.6	41.72	0.9	6513
	3	151.3	7.7	11.8	48.9	6.1	-

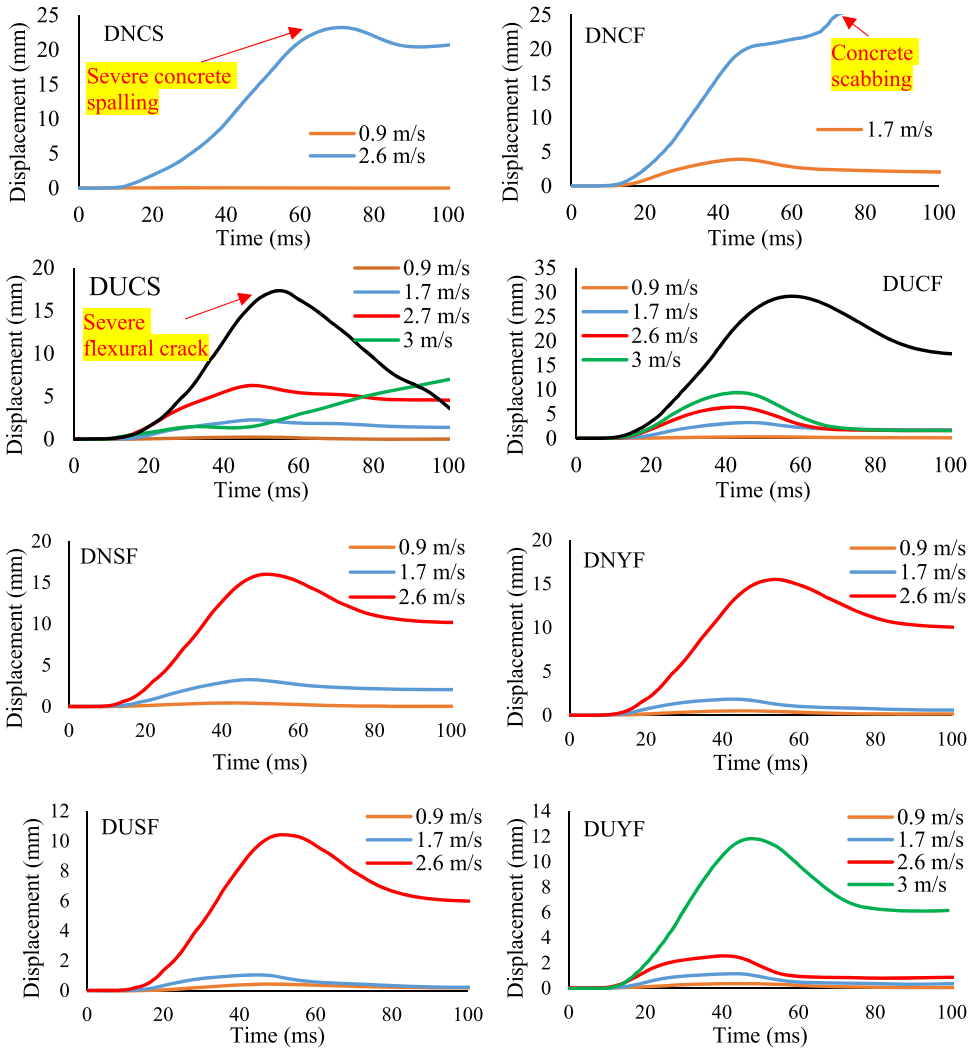

Fig. 11. Mid-span displacement time histories of decks subjected to impact loads.

displacement by 28 % from 22.2 mm to 16 mm at the impact velocity of 2.6 m/s. Similarly, for the decks with UHPC, utilizing FRP SIP formwork reduced the displacement. The displacements of decks with FRP SIP formwork under the impact velocity of 1.7 m/s were 67 % lower than the deck with FRP mesh reinforcement. Similarly, the residual displacements of Decks DUSF and DUYF were 78 % and 81 % lower than that the control Deck DUCF.

3.4.4. *Influence of Stiffener configuration*

Comparison between different types of FRP SIP formworks showed that the Y-shaped stiffened FRP SIP formwork deck led to a significantly lower displacement than the SHS stiffened SIP formwork deck even though the cross-sectional areas of these two stiffeners were similar, indicating that the Y-shaped formwork design could provide superior impact resistance. This observation is similar to its deformation performance under static loads. For normal-strength concrete, the results showed that the displacement of Deck DNYF was 44 % lower than Deck DNSF at the impact velocity of 1.7 m/s. However, this difference reduced to 3 % as both the decks failed under punching shear and impactor penetrated into the deck.

Interestingly, a comparison between UHPC decks with different types of FRP SIP formworks showed that the Y-shaped stiffened FRP SIP formwork deck exhibited a similar displacement as compared to the SHS stiffened SIP formwork deck before failure and final impact. The displacement, as mentioned earlier, was significantly influenced by the utilization of UHPC. Additionally, the potential benefits of incorporating FRP SIP formwork within UHPC were overshadowed by the dominant influence exerted by UHPC itself.

3.5. *Strain characteristics*

For RC specimens subjected to impact loads, the apparent strength of concrete can increase with strain rate. This phenomenon can be defined by the dynamic increase factor, which is a function of strain rate; therefore, the strain rate is an important property in dynamic tests. However, defining a representative strain rate for an entire structural specimen is not possible because all elements of the specimen have different strain rates simultaneously. Hence, in this study, only the maximum mid-span strain values on tensile zone of the specimens are presented as reference values, which can describe the characteristics of specimens during the impact test.

Strain gauges attached to the centre of all the decks and the maximum strain values are tabulated in Table 5. For all the RC decks, except SNCF, the strain gauge failed after 1st impact due to flexural crack of concrete at the mid-span. The strain gauge failed at the second impact for Deck SNCF. A comparison between Decks DNCS and DUCS shows that using UHPC can significantly reduce strain in concrete in the tensile zone. This is attributed to the existence of fibres which can resist and distribute stress in concrete.

The impact velocity had a direct effect on increasing the maximum

strain in the decks with FRP SIP formwork, regardless of the stiffener configuration. UHPC has a remarkable influence on reducing the strain value. For example, the maximum strains of Deck DNSF at impact velocities of 0.9, 1.7, and 2.6 m/s were 1008, 4330, and 6556 μm/m, while the strain for the corresponding deck with UHPC at similar impact velocity was 452, 1848, 3677 μm/m, respectively. As reported in the previous study [22], the nominal rupture strain of GFRP plate is 17, 000 μm/m. The low strain value of GFRP plates is due to its low modulus and over-reinforced section which led to low utilization of this material. Therefore, FRP SIP formworks with smaller thickness plates can be considered. Interestingly, the results indicated that decks with Y-shaped stiffeners exhibited slightly higher strains compared to decks with SHS stiffeners. Considering a lower displacement in the decks with Y-shaped stiffeners as compared to the one with SHS stiffeners and similar impact velocity and concrete properties, it can be inferred that the Y-shaped stiffeners make a better contribution to the member's performance under impact forces with better resistance capacities to the impact loads.

3.6. Residual capacities after impact damage

After the impact tests, Decks DUCF, DUSF and DUYF were subjected to static tests to quantify their residual load-carrying capacity. All the testing conditions were kept the same as the previous studies under static loads [6,22]. Fig. 12 exhibits the residual flexural behaviour of these three UHPC decks after the impact tests. All the decks failed under punching shear similar to their static tests. Compared to undamaged samples [6], the peak load of Decks DUCF, DUSF and DUYF reduced from 194 kN to 73 KN, 149 kN to 78 kN, and 231 kN to 203 kN, respectively. Deck DUCF showed the largest reduction in the bending capacity, followed by the deck with SHS stiffeners and then the deck with Y-shape stiffeners. Deck DUYF comprising Y-shape stiffeners exhibited a better residual loading capacity after impacts due to the use of the Y-shape stiffeners, which provided remarkable dowel action and shear reinforcement to the deck after the appearance of shear cracks. According to Nelson and Fam [5], the equivalent service load for a 1:2.75 scaled bridge deck was 24.3 kN. The residual peak loads of Decks UHPC in this study were 2.9 – 8.4 times higher than the established design service load. Deck DUYF showed a much higher moment capacity than the other decks due to the remarkable bending performance of Y-shaped stiffener in FRP SIP formworks as also observed in the previous study [6].

After the tests, the specimens were sectioned through longitudinal and transverse directions, as shown in Fig. 13. The GFRP bars, Y-shape and SHS stiffeners experienced tension-shear-coupling failure associated with the tension shear cracks within the shear zone. Sufficient bonding was observed for Deck DUSF which led to deforming and rupturing of the hollow section due to its low shear capacity. A similar behaviour was also reported for the decks with SHS stiffened formworks under static loading due to the reduction of the effective depth of the deck after failure of SHS stiffeners.

The bonding interface between stiffeners and GFRP plates has a vital role to hold the formwork so that the deck acts as a composite structure. Unlike the static test, partial debonding between concrete and the bottom plate was also observed on Deck DUYF, while significant debonding was observed for Deck DUSF. Rupture of the Y-shape stiffeners at the junction of the web and the top flanges was also observed.

Detailed observations revealed that the utilization of FRP SIP formwork with Y-shape stiffeners exhibited exceptional impact performance, surpassing that of decks with SHS stiffeners under impact loading. Additionally, the integrity of decks with Y-shape stiffeners was significantly better than decks with SHS stiffeners under impact loading.

4. Conclusion

This study investigated the performance of eight decks under sequent impact loading. The decks were divided into two sets of specimens. One set of the decks was reinforced by the internal steel rebar/GFRP bar at the tensile zone, and the other set was reinforced by FRP-SIP formworks. Additionally, the impact performance of UHPC vs normal strength concrete on deck responses was also investigated. The following remarks can be made as follows:

1) The use of GFRP bar reinforcements instead of steel reinforcement resulted in a shift in the failure mode under impact loading, e.g., from flexure to shear. The use of UHPC as compared to normal strength concrete did not change the general failure modes, e.g., localized concrete punching on the top surface, accompanied by flexural cracks around the impact region although the loading capacity was greatly increased. Additionally, flexural-shear cracks were observed closer to the support regions of the decks. Similar to the static loading test, utilizing of UHPC significantly reduced cracking and scabbing failure.
2) FRP SIP formwork demonstrated a significant reduction in deck damage by mitigating scabbing failure under impact loads. The configuration of FRP SIP formwork had a substantial influence on the impact force. Similar to the static test, the proposed Y-shape stiffened formwork exhibited higher loading capacity as compared to SHS stiffened formworks due to the increased shear resistance even though the cross-sectional area of these two stiffeners was similar.
3) The decks constructed with UHPC experienced remarkably low displacement response than those with normal strength concrete. This phenomenon was also observed for the decks with FRP SIP

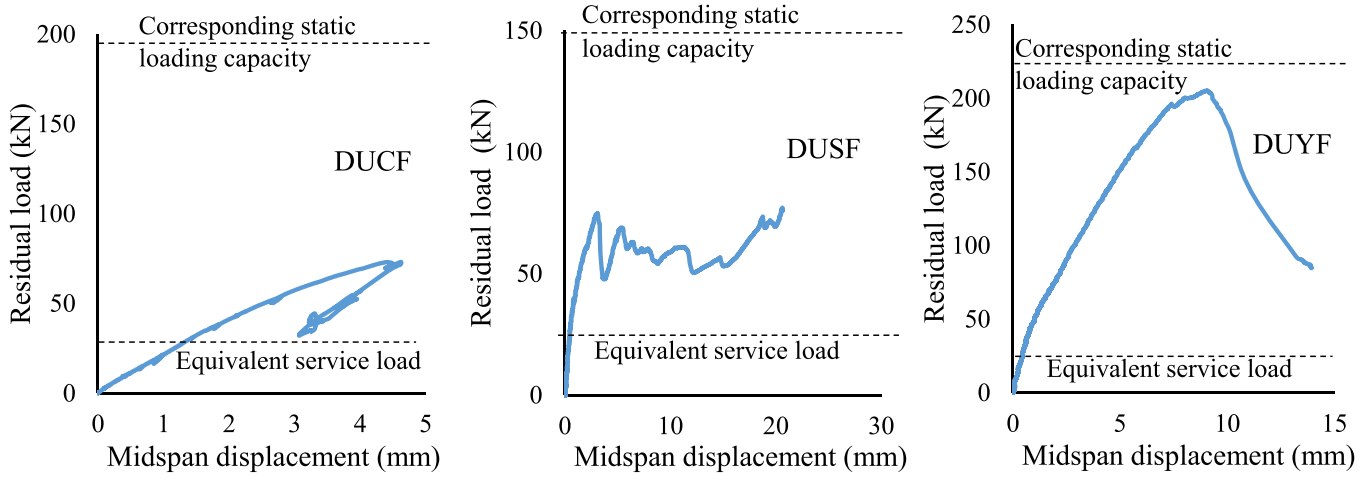

Fig. 12. Residual load-displacement relations.

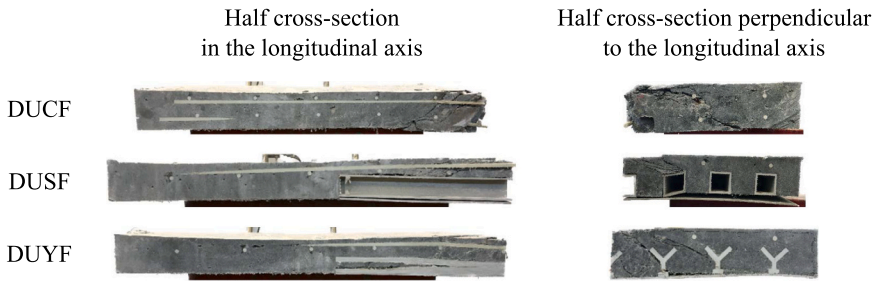

Fig. 13. Cross-section cut after test.

formworks. Notably, when GFRP bar reinforcements were replaced with Y-shaped stiffened SIP formwork, a substantial reduction of over 50 % in the maximum displacement was achieved, indicating that the use of Y-shaped stiffened SIP formwork could significantly improve the structural resistance capacity. Additionally, it was observed that the efficacy of utilizing FRP SIP formwork within the UHPC framework was undermined by the dominant influence of UHPC on deck's displacement.

4) The decks constructed with UHPC exhibited great reductions in both maximum and residual displacements, up to 70 % decrease when compared to decks made with normal strength concrete. This substantial reduction in the displacement can be primarily attributed to the remarkable influence of fibres, which significantly enhance the performance of UHPC under impact loads.
5) A new phenomenon about the impact force and reaction force was observed, i.e., the reaction forces could be greater than impact force at high impact velocities due to the activation of high vibration modes.

CRediT authorship contribution statement

Hong Hao: Funding acquisition, Supervision, Writing – review & editing. **Emad Pournasiri:** Conceptualization, Data curation, Formal analysis, Investigation, Methodology, Visualization, Writing – original draft. **Thong Pham:** Conceptualization, Methodology, Project administration, Supervision, Writing – review & editing.

Declaration of Competing Interest

The authors declare no conflict of interests.

Data Availability

Data will be made available on request.

Acknowledgements

The financial support from the Australian Research Council (Laureate Fellowships FL180100196) is acknowledged. The authors wish to thank Perma Composites Pty Ltd, Sika Australia Pty Ltd and Silicon Metal Company of Australia (SIMCOA) for providing the required material for this study.

References

[1] Remy O, Verbruggen S, Wastiels J, Tysmans T. Cement composite stay-in-place formwork: a concept for future building systems. 18th Int Conf Compos Mater (ICCM-18) Jeju Isl, Korea 2011.
[2] Akhand AM, Wan Badaruzzaman WH, Wright HD. Combined flexure and web crippling strength of a low-ductility high strength steel decking: experiment and a finite element model. Thin Walled Struct 2004;42:1067–82.
[3] Cheng Z, Zhang Q, Bao Y, Deng P, Wei C, Li M. Flexural behavior of corrugated steel-UHPC composite bridge decks. Eng Struct 2021;246:113066.
[4] Nelson MS, Fam AZ, Busel JP, Bakis CE, Nanni A, Bank LC, et al. FRP stay-in-place structural forms for concrete bridge decks: a state-of-the-art review. Acids Struct J 2014;111:1069–80.
[5] Nelson M, Fam A. Full bridge testing at scale constructed with novel FRP stay-in-place structural forms for concrete deck. Constr Build Mater 2014;50:368–76.
[6] Pournasiri E, Pham TM, Hao H. Behavior of ultrahigh-performance concrete bridge decks with new Y-shape FRP stay-in-place formworks. J Compos Constr 2022;26:04022023.
[7] Nicoletta B, Woods J, Gales J, Fam A. Postfire performance of GFRP stay-in-place formwork for concrete bridge decks. J Compos Constr 2019;23:04019015.
[8] Zuo Y, Liu Y, He J. Experimental investigation on hybrid GFRP-concrete decks with T-shaped perforated ribs subjected to negative moment. Constr Build Mater 2018;158:728–41.
[9] He J, Liu Y, Chen A, Dai L. Experimental investigation of movable hybrid GFRP and concrete bridge deck. Constr Build Mater 2012;26:49–64.
[10] Nelson M, Beriker E, Fam A. Splices of FRP stay-in-place structural forms in concrete bridge decks. J Compos Constr 2014;18:04014001.
[11] Nelson M, Eldridge A, Fam A. The effects of splices and bond on performance of bridge deck with FRP stay-in-place forms at various boundary conditions. Eng Struct 2013;56:509–16.
[12] Zou X, Feng P, Bao Y, Wang J, Xin H. Experimental and analytical studies on shear behaviors of FRP-concrete composite sections. Eng Struct 2020;215:110649.
[13] Trevor DH, Frank JV. Behavior of steel fiber-reinforced concrete slabs under impact load. Acids Struct J 2014;111.
[14] Zineddin M, Krauthammer T. Dynamic response and behavior of reinforced concrete slabs under impact loading. Int J Impact Eng 2007;34:1517–34.
[15] Zhong H, Lyu L, Yu Z, Liu C. Study on mechanical behavior of rockfall impacts on a shed slab based on experiment and SPH–FEM coupled method. Structures 2021;33:1283–98.
[16] Daneshvar K, Moradi MJ, Ahmadi K, Hajiloo H. Strengthening of corroded reinforced concrete slabs under multi-impact loading: Experimental results and numerical analysis. Constr Build Mater 2021;284:122650.
[17] Chen W, Pham TM, Elchalakani M, Li H, Hao H, Chen L. Experimental and numerical study of basalt FRP strip strengthened RC slabs under impact loads. Int J Struct Stab Dyn 2020;20:2040001.
[18] Emami F, Kabir MZ. Performance of composite metal deck slabs under impact loading. Structures 2019;19:476–89.
[19] Graybeal B, Tanesi J. Durability of an ultrahigh-performance concrete. J Mater Civ Eng 2007;19:848–54.
[20] Park SH, Kim DJ, Ryu GS, Koh KT. Tensile behavior of ultra high performance hybrid fiber reinforced concrete. Cem Concr Compos 2012;34:172–84.
[21] Pournasiri E, Ramli M, Cheah CB. Mechanical performance of ternary cementitious composites with polypropylene fiber. Acids Mater J 2018;115:635–46.
[22] Pournasiri E, Pham TM, Hao H. Structural performance evaluation of UHPC/conventional concrete cast on new Y-shape FRP stay-in-place formwork for concrete bridge decks. Structures 2022;41:1077–91.
[23] ASTM. Standard Test Method for Compressive Strength of Cylindrical Concrete Specimens. ASTM C39/C39M-21. West Conshohocken, PA: ASTM International; 2021.
[24] ASTM. Standard test method for splitting tensile strength of cylindrical concrete specimens. ASTM C496. Philadelphia (PA): ASTM; 2017.
[25] PermaComposites. PermaStruct. Perth, WA, Australia: Perma Composites; 2022.
[26] Pultrall. V-ROD - Technical data sheet. Thetford Mines, QC, Canada: ADS Composites Group: Pultrall Inc; 2021.
[27] ASTM. Standard Specification for Deformed and Plain Carbon-Steel Bars for Concrete Reinforcement. ASTM A615/A615M. West Conshohocken, PA: ASTM International; 2020.
[28] West-System. West system 105 Resin. Molendinar, QLD, Australia: West system; 2020.
[29] Granor, Elastomeric Bearings – Pads & Strip, Series Bs. 8 Reid Street, Bayswater, Victoria 3153 Australia: Granor Rubber & Engineering; 2021.
[30] Pham TM, Chen W, Hao H. Review on impact response of reinforced concrete beams: contemporary understanding and unsolved problems. Adv Struct Eng 2021;24:2282–303.
[31] Pham TM, Hao H. Plastic hinges and inertia forces in RC beams under impact loads. Int J Impact Eng 2017;103:1–11.
[32] Pham TM, Hao Y, Hao H. Sensitivity of impact behaviour of RC beams to contact stiffness. Int J Impact Eng 2018;112:155–64.

[33] Pham TM, Hao H. Influence of global stiffness and equivalent model on prediction of impact response of RC beams. Int J Impact Eng 2018;113:88–97.
[34] Pham TM, Hao H. Effect of the plastic hinge and boundary conditions on the impact behavior of reinforced concrete beams. Int J Impact Eng 2017;102:74–85.
[35] Do TV, Pham TM, Hao H. Impact force profile and failure classification of reinforced concrete bridge columns against vehicle impact. Eng Struct 2019;183:443–58.
[36] Hao H, Tran TT, Li H, Pham TM, Chen W. On the accuracy, reliability and controllability of impact tests of RC beams. Int J Impact Eng 2021;157:103979.
[37] Jones N, Wierzbicki T. Dynamic plastic failure of a free-free beam. Int J Impact Eng 1987;6:225–40.
[38] Yi W, Zhao D, Kunnath S. Simplified approach for assessing shear resistance of reinforced concrete beams under impact loads. Acids Struct J 2016;113.